Developmental analysis and optical modelling of short cell phytoliths in Festuca exaltata (Poaceae)

Edited by: Hermann Heilmeier

Journal Pre-proof

Developmental analysis and optical modelling of short cell phytoliths in Festuca exaltata (Poaceae)

D. Attolini , L. Pattelli , S. Nocentini , D.S. Wiersma , C. Tani , A. Papini , M. Mariotti Lippi

PII: S0367-2530(23)00029-4
DOI: https://doi.org/10.1016/j.flora.2023.152239
Reference: FLORA 152239

To appear in: *Flora*

Received date: 23 March 2022
Revised date: 28 January 2023
Accepted date: 6 February 2023

Please cite this article as: D. Attolini , L. Pattelli , S. Nocentini , D.S. Wiersma , C. Tani , A. Papini , M. Mariotti Lippi , Developmental analysis and optical modelling of short cell phytoliths in Festuca exaltata (Poaceae), *Flora* (2023), doi: https://doi.org/10.1016/j.flora.2023.152239

Developmental analysis and optical modelling of short cell phytoliths in *Festuca exaltata* (Poaceae)

Attolini D.[1,2] *, Pattelli L.[3,4], Nocentini S. [3,4], Wiersma D. S.[3,4,5], Tani C.[1], Papini A. [1]*, Mariotti Lippi M. [1]

[1]Department of Biology (BIO), University of Florence, Via La Pira 4, Florence 50051, Italy

[2]Department of Antics, Philosophy and History (DAFIST), University of Genoa, Via Balbi 2, Genoa 16126, Italy

[3]Istituto Nazionale di Ricerca Metrologica (INRiM), Str. delle Cacce 91, Turin 10135, Italy

[4]European Laboratory for Non Linear Spectroscopy (LENS), University of Florence, Via Nello Carrara 1, Sesto Fiorentino (FI) 50019, Italy

[5]Department of Physics, University of Florence, via G. Sansone 1, Sesto Fiorentino (FI) 50019, Italy

*** corresponding authors:**

Davide Attolini - davide.attolini@edu.unige.it

Alessio Papini - alessio.papini@unifi.it

Highlights:

- Light microscopy, SEM and TEM morphological description of short cell phytoliths of *Festuca exaltata*
- Light-interaction modelling shows that silica-cell phytoliths do not appreciably affect light intensity in the cork-cells.
- Decreasing protein content in developing silica-cells

Summary

Short cells of Poaceae often contain a cell lumen (CL) phytolith. The aim of this investigation was to analyse the features, development and possible function of CL phytoliths in *Festuca exaltata* leaves. This study employed light microscopy (LM), scanning and transmission electron microscopy (SEM and TEM respectively). The interaction of light with these phytoliths was modeled using the Finite-Difference Frequency Domain (FDFD) method. The results showed that silica deposition begins within

a medium electron density matrix. Proteins were detected in the center of the cytoplasm in a higher amount during the young stage. This occurrence suggests that proteins may be a possible component of the matrix or at least play a role in the silica deposition. At maturity, the short cell phytoliths have peculiar morphology and positioning. These were tested numerically to verify their possible role in either conveying or deflecting light rays, showing only a negligible influence of the phytoliths on the distribution of light within the leaf. A channel apparently connects the silica and the cork cell, suggesting that the cork cells have a metabolic activity related to the metabolism of the silica cells, but possibly not exclusively related to the development.

Keywords: *Drymochloa drimeja* subsp. *exaltata*; phytolith formation; phytolith light interaction; Cork cell; cell lumen phytolith

Introduction

Phytoliths are biomineral bodies that form in plants by the deposition of inorganic compounds (silica or calcium carbonate) between / in the cell walls (CW phytoliths) or in the cell lumina (CL phytoliths); calcium oxalate, an organic compound, may also form CL phytoliths (Metcalfe and Chalk, 1983; Piperno, 2006). Most of the inorganic phytoliths are due to the deposition of amorphous silicon dioxide (silica), for which reason they are frequently defined “opaline silica bodies”.

Phytoliths present a variety of shapes and sizes, which occur in different plants, in different parts of the same plant, or even in different cells of the same tissue. However, phytoliths with the same morphology may be found in plants belonging to unrelated taxa (Rovner, 1971). Their diagnostic utility largely varies on a case by case basis: it is sometimes possible to get to the species level, but more frequently only to the level of genus, family or higher taxa.

Phytoliths are present in numerous plant families, which differ in silica concentrations on a dry weight basis. Among angiosperms, the highest level of silicification occurs in Poaceae and Arecaceae (Hodson et al., 2005), but these bodies have been found even outside seed plants (Sheue et al., 2020). Regarding Poaceae, phytoliths are found throughout the plant, mostly in the aerial part and in particular in the leaf epidermis. In these plants, the epidermis displays very distinctive features: long cells (elongated with respect to the leaf axis) and short cells (aligned to the long cells) are distributed according to different patterns, which represent significant diagnostic markers (Rudall et al., 2014). Some of the short cells may present a CL phytolith (silica cells), often of diagnostic relevance (Metcalfe, 1960; Rudall et al., 2014).

Epidermal micromorphology and phytoliths of the genus *Festuca* L. are among the most studied in the Poaceae family (e.g. Consaul and Aiken, 1993; Marx et al., 2004; Namaganda et al., 2009; Ortúñez and de la Fuente, 2010; Fernández Pepi et al., 2012; Ortúñez and Cano-Ruiz, 2013; Dani et al., 2014; Cougnon et al., 2016) and more than twenty morphotypes were described in the subgenus *Festuca* (Fernández Pepi et al., 2012). Differences were observed in shape and distribution of phytoliths in the adaxial and / or abaxial epidermis of the leaf blade, and the same morphotype may present a degree of variability in relation to the position in the blade. Most of the morphotypes are linked to the silicified walls of epidermal or vascular cells, the others occurring in the cell lumina, mainly in the bulliform cells of the abaxial blade surface and in the short cells of the entire epidermis.

The development of phytoliths in plants is a largely unknown process, despite the interest in their chemical and isotopic composition (Hodson, 2016). In-depth analyses on the silicification stages were carried out, for example, on leaf blades of Bambusoideae, collected from before the opening of the leaf blades, up to well-developed leaves, where the silicification process is complete (Motomura et al., 2000, 2002, 2004, 2006). Studies on the development of CW phytoliths indicate that silica is deposited onto carbohydrate material, even if other kinds of organic matrices cannot be ruled out. In *Selaginella*, *Equisetum* and several flowering plants, callose is one of the carbohydrates involved in the process (Waterkeyn et al., 1982; Law and Exley, 2011). Analysis of the cell wall biosynthesis in grass hairs evidenced an increase in the amount of mixed-linkage (1→3,1→4)-β-d-glucans during silica deposition (Perry et al., 1987). Pectic arabinan possibly has a role in the silicification of the walls of the epidermal idioblasts in *Adiantum* (Leroux et al., 2013). Studies on silicification of the inner tangential walls of the epidermal cells of *Sorghum bicolor* indicate the involvement of non-cellulosic cell wall polysaccharides, namely arabinoxylan–ferulic acid complexes (Soukup et al., 2013).

Regarding CL phytoliths, there is no indication of the presence of an organic matrix where silica is deposited (Hodson et al., 1985; Zhang et al., 2013). Kumar et al. (2017a) demonstrated that silica cells are viable and well connected to the neighboring cells during silica deposition in *Sorghum* and suggested that the process could be enhanced by materials such as proteins, peptides, or sugars contained in the apoplastic space. Deposition seems to begin in the cell wall, where it could be mediated by callose or lignin, before filling the cell lumen (Zhang et al., 2013). The programmed death of the silica cell is independent of the silica-deposition process: generally, silica deposition precedes cell death, which leaves a void that remains unsilicified (Kumar and Elbaum, 2018). In the palm *Syagrus coronata*, silica grains are presumably formed by the precipitation of silica in the vacuoles (Lins et al., 2002). Macromolecular assemblages containing proteins seem to be associated with

biogenic silica in *Equisetum* and *Phalaris*, even if their precise role requires further investigation. The organic material involved in the phytolith deposition possibly contains lysine, proline and serine, which would bind the silica by means of a hydrogen-bounding mechanism (Harrison, 1996; Perry and Keeling-Tucker, 2003). In general, CL phytoliths are expected to contain a larger amount of proteins, lipids and nucleic acids than the CW ones (Hodson, 2016).

Numerous hypotheses have been formulated about the function of phytoliths (Ma, 2004), but their real role is still far from being understood. A mechanical / structural function has been attributed to silica deposition, e.g. it could aid the stiffness of plant portions that are prone to structural damages or prevent the collapse of the cells (Metcalfe and Chalk, 1983; Holzhüter et al., 2003). It plays a role in water and salt exchanges, in addition to increasing the resistance to drought and other abiotic stresses, such as high temperatures and concentrations of heavy-metals (Rogalla and Römheld, 2002; Currie and Perry, 2007; Liang et al., 2007; Savvas et al., 2009; Katz, 2015, 2018; Kumar et al., 2017b; Meunier et al., 2017). It exerts a protective effect against pathogens by modulating the timing and extent of plant defense responses (Bélanger et al., 2003; Fauteux et al., 2005) and it constitutes a deterrent against herbivores (Massey et al., 2007; Hunt et al., 2008; Reynolds et al., 2009). Cork-silica cell pairs seem to be involved in the production of epicuticular wax filaments (McWhorter and Paul, 1989). Some authors have investigated the possible interaction of phytoliths with light measuring the optical properties of the whole leaf or those of the isolated phytoliths (Agarie et al., 1996; Klančnik et al., 2014; Sato et al., 2016). In rice, the typical silica cells of the epidermis are birefringent, while isolated phytoliths from long cells and bulliform cells are not. Therefore, birefringence could be due to the deposition of silica on ordered structures such as cellulose microfibrils while amorphous silica is not birefringent (Dayanandan et al., 1983). The presence of phytoliths seems to affect mainly leaf transmittance (Klančnik et al., 2014), and was suggested to possibly act as light diffusers or as "windows" that increase the photosynthesis rate (Sato et al., 2016), even if the second hypothesis is not supported by Agarie et al. (1996).

The aim of this paper is to investigate the three-dimensional morphology of the short-cell CL phytoliths, their development and interaction with light. The study was performed on *Festuca exaltata* C. Presl, Poaceae (= *Drymochloa drymeja* subsp. *exaltata* (C. Presl) Foggi & Signorini), an Italian endemic species with relatively large leaves, which grows in the beech forests of the Apennine (Conti and Bartolucci, 2015). The epidermis of *Festuca* is made up of long cells and short cells, stomata and appendages, such as prickles and uncommon hairs; bulliform cells also occur on the adaxial surface (Metcalfe, 1960; Dani et al., 2014).

This investigation aims at providing new information to answer the following questions:

a) At what stage of leaf development do silica cell phytoliths form? What is the relation between silica deposition and cell death?

b) What kind of biological matrix induce their formation (proteins, carbohydrates, lipids)?

c) What are the typical shape and position of short-cell CL phytoliths and do they affect significantly the light distribution in the mesophyll?

Materials and Methods

Festuca exaltata leaves were sampled from six living specimens belonging to the collection of *Festuca* species of Orto Botanico "Giardino dei Semplici" (Botanical Garden of the University of Florence, Italy) under the supervision of Professor Bruno Foggi, curator of the collection, who also undertook the formal identification of the plant material. A living representative voucher specimen of the species is located in the above-mentioned collection. We used also seedlings of *F. exaltata* obtained from seeds germinated on wet paper, in order to observe the first stages of development of the silica cells.

At least three fresh leaves at different stages of development were collected from the central part of the tuft of each *F. exaltata* plant, from newly emerged leaves to completely developed ones (Table 1), following Motomura et al. (2006) and Li et al. (2017). Sampling was performed in 2016–2018.

>>insert Table 1 here

Phytoliths were isolated using the dry-ashing method, which utilizes high temperatures and HNO_3 (Piperno, 2006). Several dozens of sections from the middle part of the leaf were analysed for each sample.

Light microscopy (LM) – In order to examine the shape and orientation of the silica cells, the epidermis of fresh leaves was observed by LM after peeling (Leica DM2500). Transversal and longitudinal sections were obtained with a cryomicrotome (CryoCut, American Optical Corporation), operating at -20 °C. Isolated phytoliths included in a water/glycerol 1:1 v/v solution were also observed in wet, unsealed mounts, which allowed the rotation of the phytoliths, to observe their three-dimensional shape.

Samples from the middle part of leaves at different development stages were fixed in FAA (Clark, 1973), embedded in Technovit® 7100 Kulzer and sectioned with a Leica Reichert Om-U3 Ultramicrotome. Fresh and embedded material was stained with:

- Toluidine Blue for general staining of acidic tissue components for several secondary metabolites (Trump et al., 1961; Ribeiro and Leitão, 2020)
- Aniline Black-B for proteins (Fisher, 1968)

- Aniline Blue WS for ß-glucans (Currier and Shih, 1968)
- Calcofluor for ß-glucans (Clark, 1973)
- Phloroglucinol-HCl for lignin (Jensen, 1962)
- Sudan III-IV for lipids (Jensen, 1962)
- PAS reagent for total insoluble polysaccharides (O'Brien and McCully, 1981)

Observations were carried out using Leica Leitz DMRB light microscope.

Scanning electron microscopy (SEM) – SEM analysis was carried out to observe at high level of detail the shape and position of silica, cork and long cells and the phytoliths linked to these cells. Samples from the middle part of leaves at different stages of development were fixed in FAA, dehydrated through an ascending ethanol series, subjected to Critical Point Drying and gold coated.

To investigate the 3D shape of the phytoliths, these were isolated from leaf fragments by charring at 500 °C in a muffle furnace and then gold coated for SEM observation.

Observation and Energy-Dispersive Spectroscopy (EDS) analysis were performed using a ZEISS EVO MA15 scanning electron microscope with micro-analyzer INCA Wave 250, to analyse silica distribution and its variation in leaves at different stages of development.

Transmission electron microscopy (TEM) – To investigate the ultrastructure of the cells, small pieces (2 mm × 2 mm cutting surface) of the middle part of leaves at different stages of development were fixed overnight at 4 °C in 2.5% glutaraldehyde in 0.1 M phosphate buffer at pH 7.2 and post-fixed in 2% OsO_2 in the same buffer. The samples were then dehydrated and embedded in Spurr's resin as in Mosti et al. (2013) and van Doorn and Papini (2016). Transverse sections approximately 80 nm thick were cut with a diamond knife on a Reichert-Jung ULTRACUT ultramicrotome. The sections were contrasted with uranyl acetate and lead citrate. The observations were performed with a Philips EM 201 transmission electron microscope.

Finite-Difference Frequency Domain calculations – The interaction of light with the epidermis has been modelled using an open-source implementation of the Finite-Difference Frequency Domain (FDFD) method (https://github.com/fancompute/fdfdpy). After analyzing the precise morphology of the silica cell phytolith (see above), the position of a typical phytolith in the surrounding tissues was obtained by optical micrographs of longitudinal sections of the leaf at the developed leaves (DL) stage. The segmented geometry was subsequently converted to a 2D spatial permittivity distribution assuming the typical refractive index values reported for other plant species in the literature (Woolley, 1975; Elbaum et al., 2003; Tamada et al., 2014). In particular, we assumed refractive index values of 1.48 for

the cell walls, 1.43 for the phytolith, 1.40 for the cork cell, 1.38 for the cytoplasm, 1.34 for the vacuoles and 1.0 for the air (external environment and inclusions inside the leaf). Tests were carried out considering the relative illumination angle between the leaf and the Sun to be between 10° and 30°: these values were chosen based on how *Festuca* DL are inclined with respect to the ground. For simplicity, real refractive index values are assumed in order to investigate specifically the possible role of the CL phytolith as a refractive optical element. Light intensity distributions for plane wave illumination and transverse electric (TE) polarization have been calculated over a spectral range between 600 and 700 nm and combined together to give an average response in the wavelength range of interest. Light in this wavelength range interacts with both chlorophylls and phytochromes. In particular, red light and phytochromes are involved in leaf growth and unrolling (Beevers et al., 1970; Shlumukov et al., 2001), which happens during the time span taken into consideration in this paper.

Results

The following abbreviations will be used in the next paragraphs: SE (seedling), YL (Young leaves), UL (Unrolling leaves), DL (Developed leaves).

Seedling leaf, light microscope

It was difficult to find cork cells and silica cells at a very young stage. Only a few could be observed. The cork cell was much shorter than normal epidermal cells and its vacuole was smaller than that of the epidermal cells. As a consequence of that, the cytoplasm was strongly toluidine blue positive (Fig. 1A). The nucleus and the vacuole were positioned close to the internal tangential wall (Fig. 1A). On the contrary the nucleus of the young silica cells was towards the outer tangential wall (Fig. 1A). The cork cell vacuole occupied a large part of the cytoplasm (Fig. 1B) and the young silica cell was almost completely occupied by nucleus and cytoplasm, while vacuoles were small and distributed all around the cytoplasm (Fig. 1B).

>>insert Fig. 1 here

Leaf surface analysis (adult leaf)

The abaxial surface of *F. exaltata* leaf displayed a well-defined pattern, with long cells alternate to short cell pairs: a proximal cork cell and a distal silica cell. In the peelings, the cork cells appeared transversally elongated or slightly reniform, with the concavity toward the leaf apex; the silica cells varied from elliptic – with a transversal main axis – to circular, sometimes slightly reniform, with a concavity toward the leaf apex (Fig. 2a). Silica cells could be replaced by prickles and, more rarely, by stomata.

Rows of stomata run along the leaf. In the adaxial surface, the long–short cell pattern was present on the veins; the epidermis between adjacent veins showed numerous stomata, long cells and rare small isodiametric cells; this arrangement was interrupted by the occurrence of a central row of bulliform cells. Linear 1–2 celled trichomes occurred at the leaf margin.

>>insert Fig. 2 here

LM leaf cross sections

At YL stage, LM observation revealed that the epidermis had long cells with a thick outer tangential wall (Fig. 2b,c) and a large vacuole that occupied most of the lumen (Fig. 2b). The two short cells displayed different features. Silica cells presented a very thin outer tangential wall, which seemed essentially constituted by the cuticle only (Fig. 2b) and was not stained by Calcofluor. Most part of the silica cells presented a cell lumen occupied by a rather homogeneous content, which is negative to the PAS staining (Fig. 2d), and with one to few small dark Aniline Black-B positive circular spots (Fig. 2e). The cork cells had rather thin walls, similar to the inner walls of the long cells; the cytoplasm was deeply stained by Toluidine Blue; the nucleus, located in the middle part of the cell, occupied a large part of the lumen (Fig. 2f). A narrow channel crossed the wall at the inner end of the silica cell (Fig. 2d,f).

At UL stage, the walls of the silica cells were thickened, with the exception of the outer tangential wall which was very thin and Sudan III-IV positive (Fig. 1S, Supplementary information). The cytoplasm was not detectable and a translucent deposit occupied the lumen of the silica cells. Cork cells presented thickened walls; they did not exhibit other evident changes except for an increase in size of the vacuole that occupied up to the half of the lumen.

SEM and EDS analysis

At YL and UL stages (Fig. 3a), the leaf surface presented long cells with evident margins interdigitated with those of the adjacent cell. Cork cells were hardly detectable: a slight depression appeared at the distal end of the long cell, between the long cell and the aligned silica cell. Silica cells appeared as circular shallow depression with a very thin raised edge, which may be complete or distally interrupted. Long cells displayed the same features observed at the previous stages. Clear depressions pointed out the position of the cork cells. Silica cells had a reniform, semi-circular, or rarely circular barely concave surface, surrounded by a raised edge.

Charred samples (isolated phytolith or aggregated phytoliths) offered the opportunity to observe the 3D-shape of the silica cell phytoliths and their position and orientation in the leaf (Fig. 3b). Silica cell phytoliths vaguely resembled truncated cones or a double horn anvil (Fig. 3c,d) and may be described

as “rondel” *sensu* ICPN 2.0 (ICPT, 2019). The larger base (outer periclinal surface) is commonly reniform, slightly concave, located at the level of the leaf surface. The smaller base (inner periclinal surface) is very narrow often reduced to a linear edge (Fig. 3d) (“carinate” in ICPN 2.0), and faced to the inner part of the leaf. Sometimes, the lateral surface is concave toward the leaf apex (Fig. 3a). The axis of this solid passed through the centre of the base non-perpendicularly.

>>insert Fig. 3 here

EDS analysis (Fig. 4) revealed that at YL stage silicon is detectable on the distal part of the prickles (Fig. 3Sa); silica cells exceptionally showed silicon accumulation in 8 cm-long leaves. Low values of silicon are generally recorded in the silica cells at UL stage when silicon was not yet detectable in the long cells. At DL stage, silica cells displayed high values of silicon, and silicon was also detectable on the long cell surface. Different degrees of silicification were recorded in the same leaf blade, but the tendency is evidently towards the increase in silicification proceeding from the YL to the DL stage (Fig. 4, Table 1S), even if silicification appeared to be lacking in a few silica cells at the DL stage too (lowest variation limits in Fig. 4).

>>insert Fig. 4 here

TEM analysis

At YL stage, the silica cell cytoplasm displayed some large spheroidal membrane-limited bodies made up of grey homogeneous material; RER cisternae and ribosomes were mainly located on the cuticular side of the membrane (Fig 5a,b). A dark line corresponding to a channel crossed the wall connecting the internal side of the silica cell to the adjacent cork cell (Fig. 5a). The middle lamella (observable in the internal tangential wall) was less electron transparent (Fig. 5a). The cork cell had electron dense cytoplasm, a nucleus with condensed chromatin (compare with a cell of the parenchyma in Fig. 2S) and a large vacuole (Fig. 5a).

At UL stage, the silica cell lumen was occupied by a granular matrix tending to fracture along lines orthogonal to the external wall; spheroidal membrane-limited bodies were visible in the cytoplasm (Fig. 5c). The cork cells showed a thick wall; electron dense layers were visible on the external tangential walls; the nucleus had mainly condensed chromatin. A channel apparently connected the silica cell with the cork cell (Fig. 5c), even if it is not easy to follow the channel from the start to the end, also because the TEM section is 80 nm thick, and in some points it may result cut from the plane in a curved tract.

At DL stage (Fig. 5d,e) the silica cell cytoplasm is still occupied by the granular matrix seen also in the UL stage. Apparently, the sectioning process had caused the fracturing of the silica cell content along lines orthogonal to the epidermis (Fig. 5d,e). The cork cells did not display evident changes with respect to the previous stage (Fig. 5e).

>>insert Fig. 5 here

Silica body – light interaction

In order to test the hypothesis about a possible optical role played by *F. exaltata* phytoliths, we simulated a relative illumination angle between the leaf and the Sun consistent with strong midday illumination. Fig. 6 shows the configuration for a relative angle of \theta_{leaf} - \theta_{Sun} = 20 degrees, which corresponds to, e.g., a vertical leaf illuminated by the sun at a height angle of 70 degrees, or a slightly patent leaf at an angle of 80 degrees illuminated by a Sun at 60 degrees, etc.
Different relative incidence angles have also been tested in a range of ±10° around this value, returning qualitatively similar results.

>>insert Fig. 6 here

To give a more quantitative idea on whether the presence of the phytolith can introduce a significant redistribution of the intensity within the leaf tissues and cells, one can evaluate the overall intensity change over certain regions. For instance, the relative intensity change within the cork cell area varies from 0.5% to 1.3% for incidence angles between 20° and 30° between the Sun and the leaf. The relative difference increases to 5% for 10°, which however is less significant since almost no light can penetrate into the leaf at such shallow incidence angles, and thus even small variations have a larger relative weight. All in all, the small magnitude of the observed intensity reduction introduced by the phytolith, evaluated at different incidence angles, suggests that its presence should not have any significant impact on chlorophylls and phytochromes. Fig. 6 shows, from left to right, the orientation of the representative configuration used for the simulations (Fig. 6a), a portion of longitudinal micrograph (Fig. 6b), and the segmented permittivity distribution that is fed into the simulation (Fig. 6c).
Fig. 7 shows a side-by-side comparison of the two simulations obtained with and without the phytolith, showing that the presence of the silica body does not affect appreciably the amount nor the spatial distribution of intensity under the phytolith and in the underlying parenchyma. These results suggest that the presence of phytoliths on *F. exaltata* DL is not directly related to an optical function. This is consistent with the low refractive index contrast between the silica bodies and the surrounding cell walls and cuticles.

>>insert Fig. 7 here

Discussion

The leaf epidermis of *Festuca*, as many other grasses, is made up of long and short cells (Fig. 2a), the latter developing into silica and cork cells. The precise distribution pattern opened to some questions regarding the relationship between the different cell elements and the developmental stages that lead to the final, mature structure. The silica bodies that form inside the silica cells deserve particular attention. Phytoliths in *F. exaltata* form in silica cells when the leaf is few centimeters long and still rolled. They display a peculiar shape (Fig. 3c,d), vaguely resembling an oblique truncated cone with reniform to oval larger base (the outer periclinal surface) and a smaller base (the inner periclinal surface) often reduced to a linear edge. The larger base is placed at the level of the leaf surface, the smaller one faces the inner part of the mesophyll (Fig 2c,d,f). The axis of the phytolith forms an angle of about 45° with respect to the leaf axis. In this position, the larger base of the phytolith and consequently the outer tangential wall of the silica cell covers the most part of the adjacent cork cell, which reaches the leaf surface with a small part of its outer tangential wall, reducing the area that is directly reached by light (Fig. 2d,f). This area has a semilunar shape (Fig. 2a), which is the reason for its naming collar-shape (Kaufman et al., 1970).

According to our observation, in *F. exaltata* the breakdown of the silica cell protoplast precedes the formation of the CL silica body in a very precocious stage, as also observed in *Triticum aestivum* (Blackman, 1969). In the 3 cm-long leaves (YL), silica cells already display a rather homogeneous content and organelles are hardly detectable (Fig 5a,b). Subsequently (UL stages and DL), silica deposits occur in silica cells (Fig 5c–e). Similar behavior was observed in the glumes of *Phalaris canariensis* (Hodson et al., 1985), where the cytoplasm contents of the silicified cells broke down before the emergence of the panicle. Anyway, recent research at air-scanning electron microscopy in *Sorghum* suggests that silica cells are viable during the whole process of silica deposition (Kumar et al., 2017a).

Our data indicate that the silica deposition is not perfectly synchronous in all the short cells, given that different degrees of silicification were recorded in the same leaf blade. Furthermore, silicification may even fail, as observed in wholly developed (DL) leaves. The silica deposition in short cells follows that in prickles and precedes that of long cell walls, in agreement with the results of other studies (Fig. 3S),

which indicate that the silica cells are among the first epidermis cells involved in biomineralization (Motomura et al., 2006; Fernández Honaine et al., 2016; Kumar et al., 2017b).

Regarding the phytolith formation, in *F. exaltata* silica is deposited onto a matrix that does not contain carbohydrates as shown by histochemical staining. A more or less spherical body begins to form in the silica cell already at a very young stage of the leaf and this spherical body is PAS negative (Fig. 2d). Indeed, previous studies indicated the involvement of carbohydrates within the cell lumen (Waterkeyn et al., 1982; Law and Exley, 2011), but they were not observed in other Poaceae (Hodson et al., 1985) and neither the presence of other substances that stimulate the gradual infill of the cell (Hodson, 2016). In the glume of *Phalaris canariensis,* silica granules fill the lumen of the silica cell without evidence of a matrix in the cytoplasm (Hodson et al., 1985); in the vacuoles of the palm *Syagrus coronata*, silica grains are presumably formed by the precipitation of silica, without the occurrence of template and proteins (Lins et al., 2002); in the hypodermal layer of the leaves of *S. coronata*, regularly shaped phytoliths are deposited in extracellular spaces; in the leaf of *Oryza sativa*, needle-shaped silica structures seem to arise from the inner layer of the cell wall after the wall is lignified (Zhang et al., 2013).

Conversely, in *F. exaltata* the silica cell lumen fills with a homogenous content (Fig. 4S) with Aniline Black-B positive material occupying a large part of the cytoplasm in some cells (Fig. 4Sa), while in other cells only dots are present within a more transparent material possibly already silica (Fig. 4Sb). These dots observed with histochemical methods (aniline black positivity) corresponded to the ovoidal grey bodies observed in TEM images, apparently surrounded by a possibly membraneous layer. These observations may hint at the presence of proteins as possible component of a silica deposition matrix. However, we showed different stages of accumulation of proteins in the center of the cytoplasm, but we were not able to identify a real matrix, that is a clear pattern of material with a definite shape, hence the presence of a matrix to direct the deposition of silica still needs further investigation.

Considering the fact that proteins gradually disappear during the deposition of silica, and that histochemical staining does not highlight the presence of other types of matrix, proteins may be involved in the deposition of silica, as also suggested by Kumar et al. (2020).

A narrow channel with a diameter varying from 200 nm on the silica cell side to 30–50 nm on the opposite side, apparently connects the inner side of the silica cell to the adjacent cork cell (Fig. 5c), even if it is difficult to visualize a complete structure from the start to the end. The channel might be the same as the pit connection observed between cork and silica cells of *Lolium temulentum* (Lawton,

1980: Fig. 20), and is present during the whole span of time from 3 cm-long leaves (YL) up to the complete development of the leaf blade, when the silica cells are senescent. A connection among the silica cell and the neighbouring cells was also evidenced in the young leaf of *Sorghum bicolor* (Kumar et al., 2017a).

This connection would suggest a direct involvement of the cork cell in the metabolism of the silica cell and possibly in the development of the short cell phytoliths. Notably, cork cells have dense cytoplasm, rich in ribosomes, displaying cytological features that are very different from those of the common epidermis cells, which are normally occupied by a large vacuole (Fig. 5d). This aspect suggests that they have a metabolic activity that differs from that of all the adjacent cells, both silica and long cells. Similar features were already observed in silica and cork cell pairs of the internodal epidermis of *Avena* (Kaufman et al., 1970), *Lolium* (Lawton, 1980), *Phalaris canariensis* (Hodson et al., 1985), and in *Sorghum halepense* leaves (McWhorter and Paul, 1989).

The function of silica in the epidermis cells has not been totally clarified yet, even if many studies support different hypotheses about its role, such as herbivore deterrence, drought resistance, structural support etc. Regarding structural support silica deposition seems to allow the leaf to maintain its extension even in the case of paucity of water, by increasing the rigidity of the leaf. Anyway, the silica cell phytoliths do not seem to have a structural role in supporting the leaf blade because they are spaced apart and not directly connected to other silicified structures.

A possible function may be related to the capability of the silica body to deviate light, creating shadow cones and zones with higher light exposure. This effect could affect the cork cells, which are placed under the silica cells, with only a negligible portion of their surface in direct contact with the atmosphere and sunlight. As already said, the dense cytoplasm of the cork cells denotes an intense metabolic activity possibly connected to the metabolism of the silica cells. This activity goes beyond the lifespan of the silica cells, continuing when the silica cell phytoliths are already fully formed, at DL stage. This suggests that the role of the cork cells is not exclusively related to the formation of the phytoliths, which begins before and ends after the leaf unrolling and is stimulated by red light (Beevers et al., 1970; Shlumukov et al., 2001). However, our experiments evidenced that the silica cell phytoliths do not affect appreciably the amount nor the spatial distribution of light intensity in the cork cell and the underlying parenchyma within a range of incidence angles that are representative of the typical relative orientation between the leaf blade and Sun (Fig 7, 5S–6S). As a matter of fact, the incidental details of the local surface morphology of the leaf can apparently affect the internal intensity distribution up to an even larger degree than the phytolith itself. In the simulation shown in Fig. 7, this

is seen for example looking at the concentration of light induced by the bulge surrounding the shallow depressions in correspondence of the silica cell phytoliths. This suggests that, albeit not directly, the presence of the short cell phytolith may still have an indirect influence on the internal intensity distribution through their modulation of the leaf surface morphology. Figure 7S shows a side-by-side comparison between the light distribution obtained for the original surface morphology and a case where we have manually manipulated the surface to make it more flat above the typical phytolith location. The flattened configuration is associated with a more uniform illumination of the underlying parenchyma and a significant increase (≈25%) of the intensity reaching the cork cell compared to the original configuration where light seems to be partially deflected around it. Thus, other morphological features on the leaf surface could modulate the intensity of the red light on the cells more effectively than phytoliths, possibly influencing the signal leading to leaf unrolling.

New research is needed to further investigate this perspective, by analyzing a large number of representative leaf surface samples and their full three-dimensional morphologies, which however remains challenging both experimentally and numerically due to the need to manually classify and pre-process the micrographs or microtomographs so that they can be used in the simulations, and due the large scale of the problem compared to the typical wavelengths of light. In this perspective, we should also note that silica cells present a smoother outer surface than those of the long cells, which were shown to have a role in the diffusion of the light ("silica plates" in Sato et al., 2016). On the other hand, the entire leaf surface is covered by epicuticular waxes (which were not considered at this stage of modelling) and just the cork-silica cell pair seems to be involved in the production of wax filaments (McWhorter and Paul, 1989). Despite being limited by the above modeling simplifications, our numerical outputs show that the refractive index contrast between the phytolith and its surrounding environment is too low for it to directly serve a significant optical function.

Other possible functions of the *F. exaltata* silica cell phytoliths could be generic protection against pathogens and defense against herbivorous insects, as supposed for other plants (Bélanger et al., 2003; Reynolds et al., 2009). This last hypothesis has to be taken in account, given that their presence could damage the mouth parts of the insects and may interfere with the radular teeth of Mollusca (because of their size).

Conclusions

In the leaves of *F. exaltata*, the epidermis consists of long cells alternating with pairs of short cells that differentiate into a cork cell and a silica cell. The cork cells are placed under the silica cells, with only a

negligible portion reaching the surface. Cork cells exhibit dense cytoplasm indicative of intense metabolic activity.

According to our observation, in *F. exaltata* the breakdown of the silica cell protoplast precedes the formation of the CL silica body, which happens very early in the development of the leaf. However, the collected data show that silica deposition is not perfectly synchronous in the leaf blade.

Histochemical stainings indicate the occurrence of decreasing amounts of proteins during the developmental stages of the leaves. They could represent a matrix component or be in some way involved in phytolith formation.

Cork and silica cells are apparently connected by a channel that crosses the interposed walls, suggesting a metabolic connection. The activity of the cork cells goes beyond the lifespan of the silica cells, continuing when the silica cell phytoliths are already fully formed, after the unrolling of the leaves. This suggests that the role of the cork cells is not exclusively related to the formation of the phytoliths.

Numerical calculations have shown that the presence of phytoliths does not appreciably affect the amount nor the spatial distribution of light in the underlying cells, leaving uncertainty about the precise function of these structures, which have such a peculiar shape and an ordered distribution.

Funding information - This work was supported by the University of Florence (Fondi di Ateneo per la ricerca scientifica, ex 60%).

Acknowledgments - The Authors wish to thank Prof. Bruno Foggi (University of Florence) and the Regional Nature Reserve Lecceta di Torino di Sangro (Chieti, Italy) for providing the plant material.

This study was conducted in compliance with national research guidelines. All the relevant permissions for the collection of plant material were obtained from both University of Florence and “Sistema Museale di Ateneo” (University Museum System), the institution overseeing “Orto Botanico Giardino dei Semplici”.

Declaration of interests

☐The authors declare that they have no known competing financial interests or personal relationships that could have appeared to influence the work reported in this paper.

☒The authors declare the following financial interests/personal relationships which may be considered as potential competing interests:

One of the authors (Alessio Papini) is subject editor of Flora

Credit author statement

Attolini Davide: Conceptualization, Methodology, Validation, Investigation, Writing - Original Draft, Writing - Review & Editing, Visualisation

Pattelli Lorenzo: Methodology, Validation, Investigation, Writing - Original Draft, Writing - Review & Editing, Visualisation

Nocentini Sara: Methodology, Validation, Investigation, Writing - Original Draft, Writing - Review & Editing

Wiersma Diederik Sybolt: Resources, Writing - Review & Editing, Supervision

Tani Corrado: Validation, Investigation

Papini Alessio: Methodology, Validation, Investigation, Writing - Original Draft, Writing - Review & Editing, Supervision

Mariotti Lippi Marta: Conceptualization, Methodology, Validation, Investigation, Resources, Writing - Original Draft, Writing - Review & Editing, Supervision

References

Agarie, S., Agata, W., Uchida, H., Kubota, F., Kaufman, P.B., 1996. Function of silica bodies in the epidermal system of rice (*Oryza sativa* L.): testing the window hypothesis. Journal of Experimental Botany 47, 655-660. https://doi.org/10.1093/jxb/47.5.655

Beevers, L., Loveys, B., Pearson, J.A., Wareing, P.F., 1970. Phytochrome and hormonal control of expansion and greening of etiolated wheat leaves. Planta 90, 286-294. https://doi.org/10.1007/BF00387180

Bélanger, R.R., Benhamou, N., Menzies, J.G., 2003. Cytological evidence of an active role of silicon in wheat resistance to powdery mildew (*Blumeria graminis* f. sp. *tritici*). Phytopathology 93, 402-412. https://doi.org/10.1094/PHYTO.2003.93.4.402

Blackman, E., 1969. Observations on the development of the silica cells of the leaf sheath of wheat (*Triticum aestivum*). Canadian Journal of Botany 47, 827-838. https://doi.org/10.1139/b69-120

Clark, G., 1973. Staining Procedures, IV ed. Williams & Wilkins, Baltimore, London.

Consaul, L.L., Aiken, S.G., 1993. Limited taxonomic value of palea intercostal characteristics in North American *Festuca* (Poaceae). Canadian Journal of Botany 71, 1651-1659. https://doi.org/10.1139/b93-201

Conti, F., Bartolucci, F., 2015. Discussion and Conclusion. In: Conti, F., Bartolucci, F. (Eds.), The Vascular Flora of the National Park of Abruzzo, Lazio and Molise (Central Italy), An annotated Checklist. Geobotany Studies, pp. 181-245. Springer, Cham.

Cougnon, M., Shahidi, R., Struyf, E., Van Waes, C., Reheul, D., 2016. Silica content, leaf softness and digestibility in tall fescue (*Festuca arundinacea* Schreb.). In: Roldán-Ruiz, I., Baert, J., Reheul, D. (Eds.), Breeding in a World of Scarcity, pp. 277-281. Springer, Cham. https://DOI.org/10.1007/978-3-319-28932-8_41

Currie, H.A., Perry, C.C., 2007. Silica in plants: biological, biochemical and chemical studies. Annals of Botany 100, 1383-1389. https://doi.org/10.1093/aob/mcm247

Currier, H.B., Shih, C.Y., 1968. Sieve tubes and callose in *Elodea* leaves. American Journal of Botany 55, 145-152. https://doi.org/10.1002/j.1537-2197.1968.tb06954.x

Dani, M., Farkas, Á., Cseke, K., Filep, R., Kovács, A.J., 2014. Leaf epidermal characteristics and genetic variability in Central European populations of broad-leaved *Festuca* L. taxa. Plant Systematics and Evolution 300, 431-451. https://doi.org/10.1007/s00606-013-0893-8

Dayanandan, P., Kaufman, P.B., Franklin, C.I., 1983. Detection of silica in plants. American Journal of Botany 70, 1079-1084. https://doi.org/10.1002/j.1537-2197.1983.tb07909.x

Elbaum, R., Weiner, S., Albert, R.M., Elbaum, M., 2003. Detection of burning of plant materials in the archaeological record by changes in the refractive indices of siliceous phytoliths. Journal of Archaeological Science 30, 217-226. https://doi.org/10.1006/jasc.2002.0828

Fauteux, F., Rémus-Borel, W., Menzies, J.G., Bélanger, R.R., 2005. Silicon and plant disease resistance against pathogenic fungi. FEMS Microbiology Letters 249, 1-6. https://doi.org/10.1016/j.femsle.2005.06.034

Fernández Honaine, M., Benvenuto, M.L., Borrelli, N.L., Osterrieth, M., 2016. Early silicification of leaves and roots of seedlings of a panicoid grass grown under different conditions: anatomical relations and structural role. Plant Biology 18, 1025-1030. https://doi.org/10.1111/plb.12488

Fernández Pepi, M.G., Zucol, A.F., Arriaga, M.O., 2012. Comparative phytolith analysis of *Festuca* (Pooideae: Poaceae) species native to Tierra del Fuego, Argentina. Botany 90, 1113-1124. https://doi.org/10.1139/b2012-070

Fisher, D.B., 1968. Protein staining of ribboned epon sections for light microscopy. Histochemie 16, 92-96. https://doi.org/10.1007/BF00306214

Harrison, C.C., 1996. Evidence for intramineral macromolecules containing protein from plant silicas. Phytochemistry 41, 37-42. https://doi.org/10.1016/0031-9422(95)00576-5

Hodson, M.J., 2016. The development of phytoliths in plants and its influence on their chemistry and isotopic composition. Implication for palaeoecology and archaeoecology. Journal of Archaeological Science 68, 62-69. https://doi.org/10.1016/j.jas.2015.09.002

Hodson, M.J., Sangster, A.G., Parry, D.W., 1985. An ultrastructural study on the developmental phases and silicification of the glume of *Phalaris canariensis* L. Annals of Botany 55, 649-655. https://doi.org/10.1093/oxfordjournals.aob.a086944

Hodson, M.J., White, P.J., Mead, A., Broadley, M.R., 2005. Phylogenetic variation in the silicon composition of plants. Annals of Botany 96, 1027-1046. https://doi.org/10.1093/aob/mci255

Holzhüter, G., Narayanan, K., Gerber, T., 2003. Structure of silica in *Equisetum arvense*. Analytical and Bioanalytical Chemistry 376, 512-517. https://doi.org/10.1007/s00216-003-1905-2

Hunt, J.W., Dean, A.P., Webster, R.E., Johnson, G.N., Ennos, A.R., 2008. A novel mechanism by which silica defends grasses against herbivory. Annals of Botany 102, 653-656. https://doi.org/10.1093/aob/mcn130

ICPT (International Committee for Phytolith Taxonomy), 2019. International Code for Phytolith Nomenclature (ICPN) 2.0, Annals of Botany 124, 189–199

Jensen, W.A., 1962. Botanical Histochemistry. W.H. Freeman and Co, San Francisco, London.

Katz, O., 2015., Silica phytoliths in angiosperms: phylogeny and early evolutionary history. New Phytologist 208, 642-646.

Katz, O., 2018. Silicon content is a plant functional trait: implications in a changing world. Flora 254, 88-94.

Kaufman, P.B., Petering, L.B., Smith, J.G., 1970. Ultrastructural development of cork-silica cell pairs in *Avena* internodal epidermis. Botanical Gazette 131, 173-185. https://doi.org/10.1086/336529

Klančnik, K., Vogel-Mikuš, K., Gaberščik, A., 2014. Silicified structures affect leaf optical properties in grasses and sedge. Journal of Photochemistry and Photobiology B: Biology 130, 1-10. https://doi.org/10.1016/j.jphotobiol.2013.10.011

Kumar, S., Elbaum, R., 2018. Interplay between silica deposition and viability during the life span of sorghum silica cells. New Phytologist 217, 1137-1145. https://doi.org/10.1111/nph.14867

Kumar, S., Adiram-Filiba, N., Blum, S., Sanchez-Lopez, J.A., Tzfadia, O., Omid, A., Volpin, H., Heifetz, Y., Goobes, G., Elbaum, R., 2020. Siliplant1 protein precipitates silica in sorghum silica cells. Journal of Experimental Botany 71, 6830-6843.

Kumar, S., Milstein, Y., Brami, Y., Elbaum, M., Elbaum, R., 2017a. Mechanism of silica deposition in *Sorghum* silica cells. New Phytologist 213, 791-798. https://doi.org/10.1111/nph.14173

Kumar, S., Soukup, M., Elbaum, R., 2017b. Silicification in grasses: variation between different cell types. Frontiers in Plant Science 8, 438. https://doi.org/10.3389/fpls.2017.00438

Law, C., Exley, C., 2011. New insight into silica deposition in horsetail (*Equisetum arvense*). BMC Plant Biology 11, 112. https://doi.org/10.1186/1471-2229-11-112

Lawton, J.R., 1980. Observations on the structure of epidermal cells, particularly the cork and silica cells, from the flowering stem internode of *Lolium temulentum* L. (Gramineae). Botanical Journal of the Linnean Society 80, 161-177. https://doi.org/10.1111/j.1095-8339.1980.tb01663.x

Leroux, O., Leroux, F., Mastroberti, A.A., Santos-Silva, F., Van Loo, D., Bagniewska-Zadworna, A., Hoorebeke, L.V., Bals, S., Popper, Z.A., de Araujo Mariath, J.E., 2013. Heterogeneity of silica and glycan-epitope distribution in epidermal idioblast cell walls in *Adiantum raddianum* laminae. Planta 237, 1453-1464. https://doi.org/10.1007/s00425-013-1856-6

Li, R., Fan, J., Carter, J., Jiang, N., Gu, Y., 2017. Monthly variations of phytoliths in the leaves of the bamboo *Dendrocalamus ronganensis* (Poaceae: Bambusoideae). Review of Palaeobotany and Palynology 246, 62-69. https://doi.org/10.1016/j.revpalbo.2017.06.006

Liang, Y., Sun, W., Zhu, Y.G., Christie, P., 2007. Mechanisms of silicon-mediated alleviation of abiotic stresses in higher plants: a review. Environmental Pollution 147, 422-428. https://doi.org/10.1016/j.envpol.2006.06.008

Lins, U., Barros, C.F., Da Cunha, M., Miguens, F.C., 2002. Structure, morphology, and composition of silicon biocomposites in the palm tree *Syagrus coronata* (Mart.) Becc. Protoplasma 220, 89-96. https://doi.org/10.1007/s00709-002-0036-5

Ma, J.F., 2004. Role of silicon in enhancing the resistance of plants to biotic and abiotic stresses. Soil Science and Plant Nutrition 50, 11-18. https://doi.org/10.1080/00380768.2004.10408447

Marx, R., Lee, D.E., Lloyd, K.M., Lee, W.G., 2004. Phytolith morphology and biogenic silica concentrations and abundance in leaves of *Chionochloa* (Danthonieae) and *Festuca* (Poeae) in New Zealand. New Zealand Journal of Botany 42, 677-691. https://doi.org/10.1080/0028825X.2004.9512919

Massey, F.P., Ennos, A.R., Hartley, S.E., 2007. Herbivore specific induction of silica-based plant defences. Oecologia 152, 677-683. https://doi.org/10.1007/s00442-007-0703-5

McWhorter, C.G., Paul, R.N., 1989. The involvement of cork-silica cell pairs in the production of wax filaments in Johnsongrass (*Sorghum halepense*) leaves. Weed Science 37, 458-470. https://doi.org/10.1017/S0043174500072222

Metcalfe, C.R., 1960. Anatomy of the Monocotyledons I. Gramineae. Clarendon Press, Oxford.

Metcalfe, C.R., Chalk, L., 1983. Anatomy of the Dicotyledons. Vol II, 2nd edn. Clarendon Press, Oxford.

Meunier, J.D., Barboni, D., Anwar-ul-Haq, M., Levard, C., Chaurand, P., Vidal, V., Grauby, O., Huc, R., Laffont-Schwob, I., Rabier, J., Keller, C., 2017. Effect of phytoliths for mitigating water stress in durum wheat. New Phytologist 215, 229-239. https://doi.org/10.1111/nph.14554

Mosti, S., Ross Friedman, C., Pacini, E., Brighigna, L., Papini, A., 2013. Nectary ultrastructure and secretory modes in three species of *Tillandsia* L. (Bromeliaceae) that have different pollinators. Botany 91, 786–798. https://doi.org/10.1139/cjb-2013-0126

Motomura, H., Fujii, T., Suzuki, M., 2000. Distribution of silicified cells in the leaf blades of *Pleioblastus chino* (Franchet et Savatier) Makino (Bambusoideae). Annals of Botany 85, 751-757. https://doi.org/10.1006/anbo.2000.1124

Motomura, H., Mita, N., Suzuki, M., 2002. Silica accumulation in long-lived leaves of *Sasa veitchii* (Carrière) Rehder (Poaceae–Bambusoideae). Annals of Botany 90, 149-152. https://doi.org/10.1093/aob/mcf148

Motomura, H., Fujii, T., Suzuki, M., 2004. Silica deposition in relation to ageing of leaf tissues in *Sasa veitchii* (Carriere) Rehder (Poaceae: Bambusoideae). Annals of Botany 93, 235-248. https://doi.org/10.1093/aob/mch034

Motomura, H., Fujii, T., Suzuki. M., 2006. Silica deposition in abaxial epidermis before the opening of leaf blades of *Pleioblastus chino* (Poaceae, Bambusoideae). Annals of Botany 97, 513-519. https://doi.org/10.1093/aob/mcl014

Namaganda, M., Krekling, T., Lye, K.A., 2009. Leaf anatomical characteristics of Ugandan species of *Festuca* L. (Poaceae). South African Journal of Botany 75, 52-59. https://doi.org/10.1016/j.sajb.2008.07.004

O'Brien, S.P., McCully, M.E., 1981. The Study of Plant Structure Principles and Selected Methods. Termarcarphi Pty. Ltd., Melbourne, Australia.

Ortúñez, E., Cano-Ruiz, J., 2013. Epidermal micromorphology of the genus *Festuca* L. subgenus *Festuca* (Poaceae). Plant Systematics and Evolution 299, 1471-1483. https://doi.org/10.1007/s00606-013-0809-7

Ortúñez, E., de la Fuente, V., 2010. Epidermal micromorphology of the genus *Festuca* L. (Poaceae) in the Iberian Peninsula. Plant Systematics and Evolution 284, 201-218. https://doi.org/10.1007/s00606-009-0248-7

Perry, C.C., Keeling-Tucker, T., 2003. Model studies of colloidal silica precipitation using biosilica extracts from *Equisetum telmateia*. Colloid and Polymer Science 281, 652-664. https://doi.org/10.1007/s00396-002-0816-7

Perry, C.C., Williams, R.J., Fry, S.C., 1987. Cell wall biosynthesis during silicification of grass hairs. Journal of Plant Physiology 126, 437-448. https://doi.org/10.1016/S0176-1617(87)80028-7

Piperno, D., 2006. Phytoliths: a Comprehensive Guide for Archaeologists and Paleoecologists. AltaMira Press, Lanham (Maryland).

Reynolds, O.L., Keeping, M.G., Meyer, J.H., 2009. Silicon-augmented resistance of plants to herbivorous insects: a review. Annals of Applied Biology 155, 171-186. https://doi.org/10.1111/j.1744-7348.2009.00348.x

Ribeiro, V.C., Leitão, C.A., 2020. Utilisation of Toluidine blue O pH 4.0 and histochemical inferences in plant sections obtained by free-hand. Protoplasma 257, 993-1008. https://doi.org/10.1007/s00709-019-01473-0

Rogalla, H., Römheld, V., 2002. Role of leaf apoplast in silicon-mediated manganese tolerance of *Cucumis sativus* L. Plant, Cell & Environment 25, 549-555. https://doi.org/10.1046/j.1365-3040.2002.00835.x

Rovner, I., 1971. Potential of opal phytoliths for use in paleoecological reconstruction. Quaternary research 1, 343-359. doi:10.1016/0033-5894(71)90070-6

Rudall, P.J., Prychid, C.J., Gregory, T., 2014. Epidermal patterning and silica phytoliths in grasses: an evolutionary history. The Botanical Review 80, 59-71. https://doi.org/10.1007/s12229-014-9133-3

Sato, K., Yamauchi, A., Ozaki, N., Ishigure, T., Oaki, Y., Imai, H., 2016. Optical properties of biosilicas in rice plants. RSC Advances 6, 109168-109173. doi: 10.1039/C6RA24449A

Savvas, D., Giotis, D., Chatzieustratiou, E., Bakea, M., Patakioutas, G., 2009. Silicon supply in soilless cultivations of zucchini alleviates stress induced by salinity and powdery mildew infections. Environmental and Experimental Botany 65, 11-17. https://doi.org/10.1016/j.envexpbot.2008.07.004

Sheue, C.R., Liu, J.W., Liu, H.Y., Kuo-Huang, L.L., Chesson, P., Chen, J., Shih, M.-C., Kiew, R., 2020. Silica bodies of *Selaginella erythropus*: Detection, morphology and development. Flora 264, 151558. https://doi.org/10.1016/j.flora.2020.151558

Shlumukov, L.R., Barro, F., Barcelo, P., Lazzeri, P., Smith, H., 2001. Establishment of far-red high irradiance responses in wheat through transgenic expression of an oat phytochrome A gene. Plant, Cell & Environment 24, 703-712. https://doi.org/10.1046/j.1365-3040.2001.00718.x

Soukup, M., Martinka, M., Bosnić, D., Čaplovičová, M., Elbaum, R., Lux, A., 2017. Formation of silica aggregates in sorghum root endodermis is predetermined by cell wall architecture and development. Annals of Botany 120, 739-753. https://doi.org/10.1093/aob/mcx060

Tamada, Y., Murata, T., Hattori, M., Oya, S., Hayano, Y., Kamei, Y., Hasebe, M., 2014. Optical property analyses of plant cells for adaptive optics microscopy. International Journal of Optomechatronics 8, 89-99. https://doi.org/10.1080/15599612.2014.901455

Trump, B.F., Smuckler, E.A., Benditt, E.P., 1961. A method for staining epoxy sections for light microscopy. Journal of Ultrastructure Research 5, 343-348.

van Doorn, W.G., Papini, A., 2016. Plastid degeneration in *Tillandsia albida* (Bromeliaceae) and *Lobivia rauschii* (Cactaceae) provides evidence about the origin and destiny of multilamellar bodies in plants. Phytomorphology 66, 103-112. https://doi.org/10.1016/S0022-5320(61)80011-7

Waterkeyn, L., Bienfait, A., Peeters, A., 1982. Callose et silice épidermiques: rapports avec la transpiration cuticulaire. La Cellule 73, 267-287.

Woolley, J.T., 1975. Refractive index of soybean leaf cell walls. Plant Physiology 55, 172-174. https://doi.org/10.1104/pp.55.2.172

Zhang, C., Wang, L., Zhang, W., Zhang, F., 2013. Do lignification and silicification of the cell wall precede silicon deposition in the silica cell of the rice (*Oryza sativa* L.) leaf epidermis? Plant and Soil 372, 137-149. https://doi.org/10.1007/s11104-013-1723-z

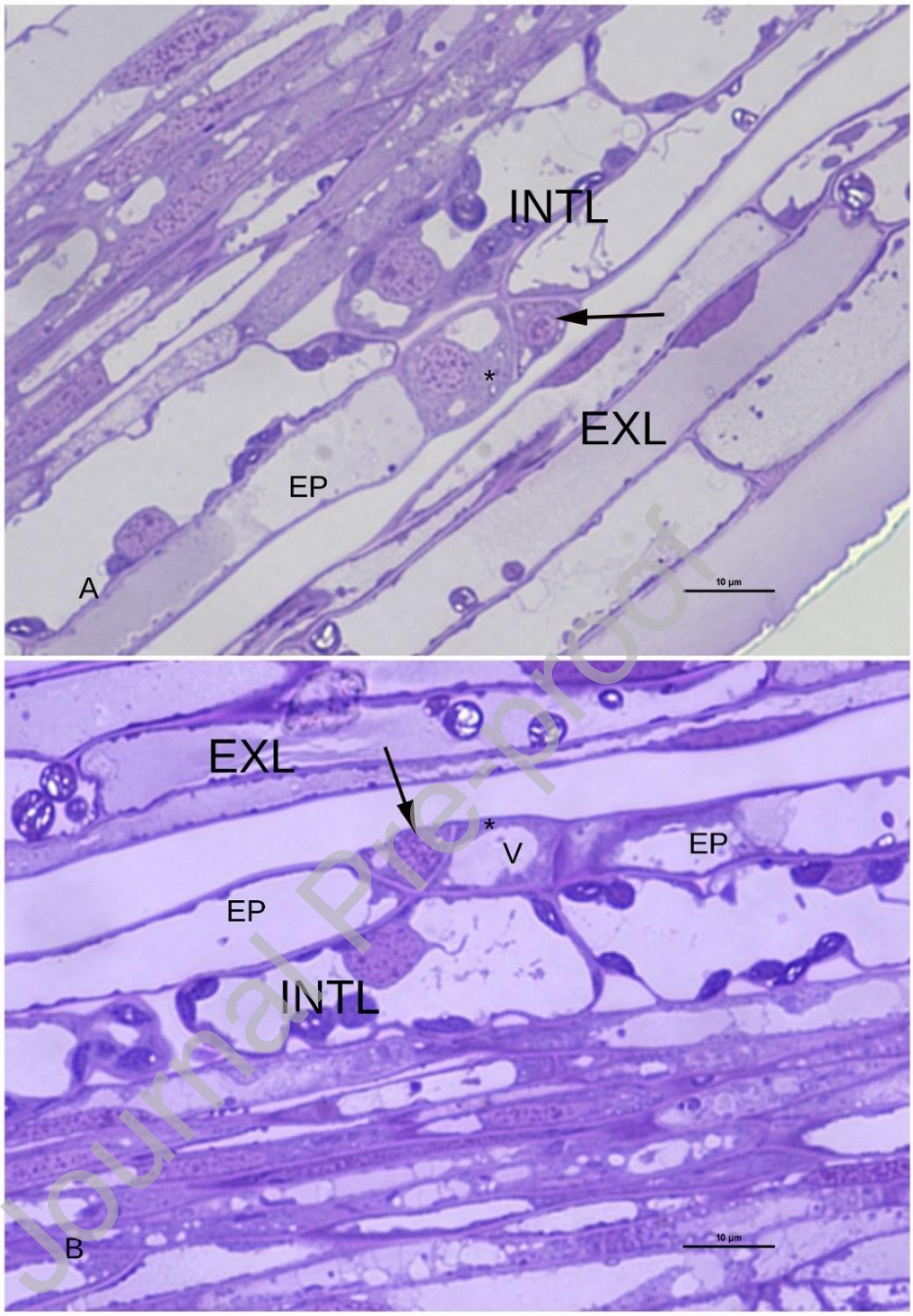

Fig. 1 LM observations on *Festuca exaltata* leaves in a seedling, Toluidine blue staining. More leaves are enveloping the stem. In the image a more external leaf (EXL) is covering a more internal leaf (INTL). A) The cork cell (asterisk) is much shorter and its vacuole smaller than in normal epidermal cells (EP). The cytoplasm is strongly toluidine blue positive. The nucleus of the young silica cell (arrow) is towards the outer tangential wall. B) Depending on the section, the cork cell (asterisk) vacuole (V) may occupy a large part of the cytoplasm, while the young silica cell (arrow) is almost completely occupied by nucleus and cytoplasm, while vacuoles are small and distributed all around the cytoplasm.

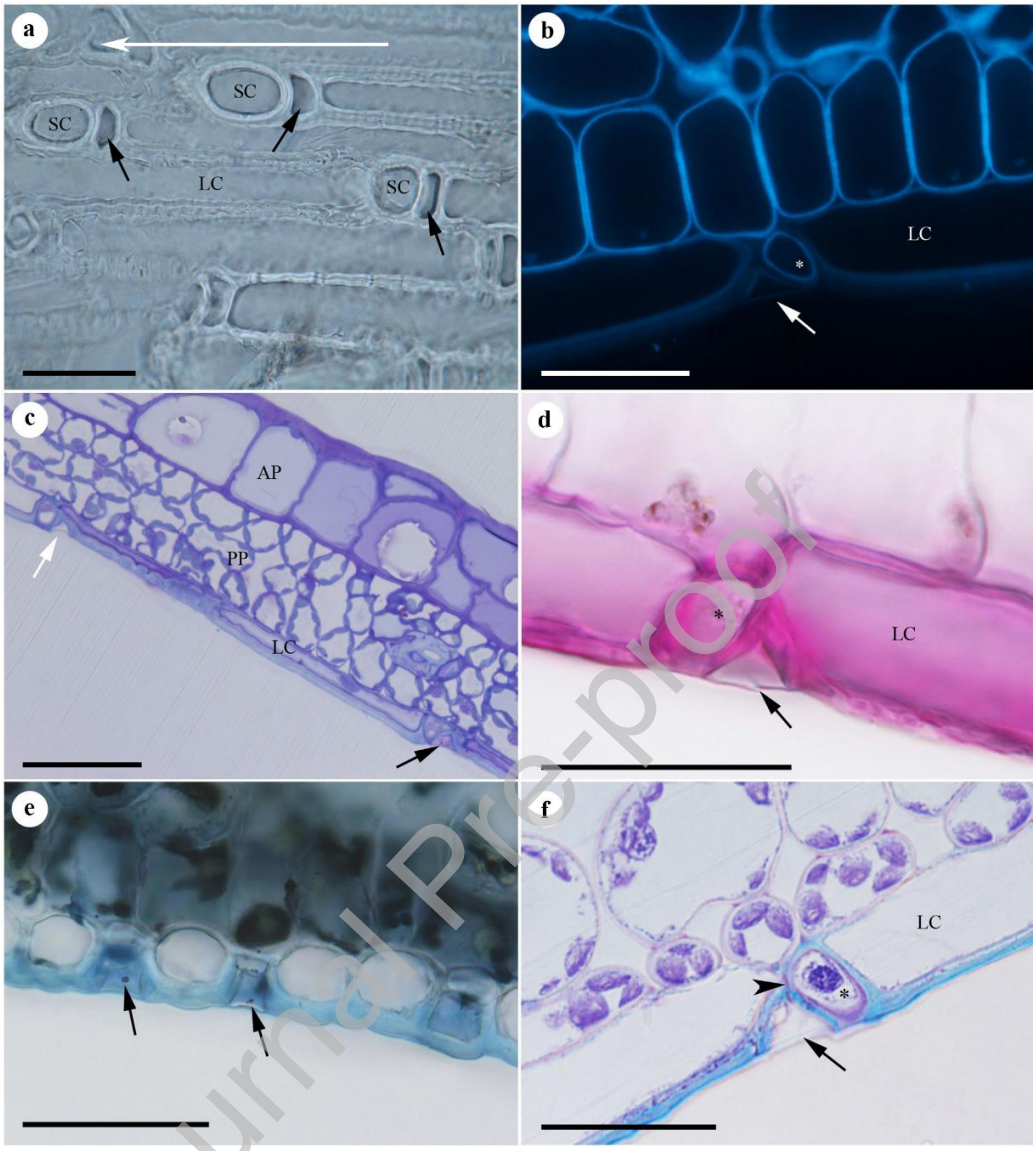

Fig. 2. LM observations on *Festuca exaltata* leaf, abaxial epidermis. (a) Abaxial epidermis from above. The white arrow indicates the position of the leaf apex. The disposition of the long cells (LC) with respect to the cork cells (CC, black arrow) and the silica cells (SC) is shown. Phase-contrast. Bar = 25 μm. (b) Longitudinal cross-section. The disposition of the long cells with respect to the cork cells (asterisk) and the silica cells (arrow) is shown. Calcofluor. Bar = 25 μm. (c) Longitudinal cross-section. Some silica cells are Toluidine blue positive (black arrow, proteins present) and others are not (white arrow, cytoplasm content mainly composed of silica). PP = Palisade Parenchyma, AP = Adaxial Parenchyma. Toluidine Blue. Bar = 50 μm. (d) Longitudinal cross-section. Silica cells (arrow) are PAS negative, evidence that they do not contain carbohydrates. PAS reaction. Bar = 25 μm. (e) Transversal cross-section. In some silica cells, a dark roundish blot (arrows), positive to the staining, is visible at the center of the cytoplasm. Aniline Black-B. Bar = 50 μm. (f) Longitudinal cross-section. In silica cells, the external wall is lacking the positivity to the stain that is continuous on the rest of the epidermis. Hence, cuticle (arrow) is apparently lacking on silica cells. A narrow channel (arrowhead) crosses the wall at the inner end of the silica cell. Toluidine Blue, LM. Bar = 25 μm.

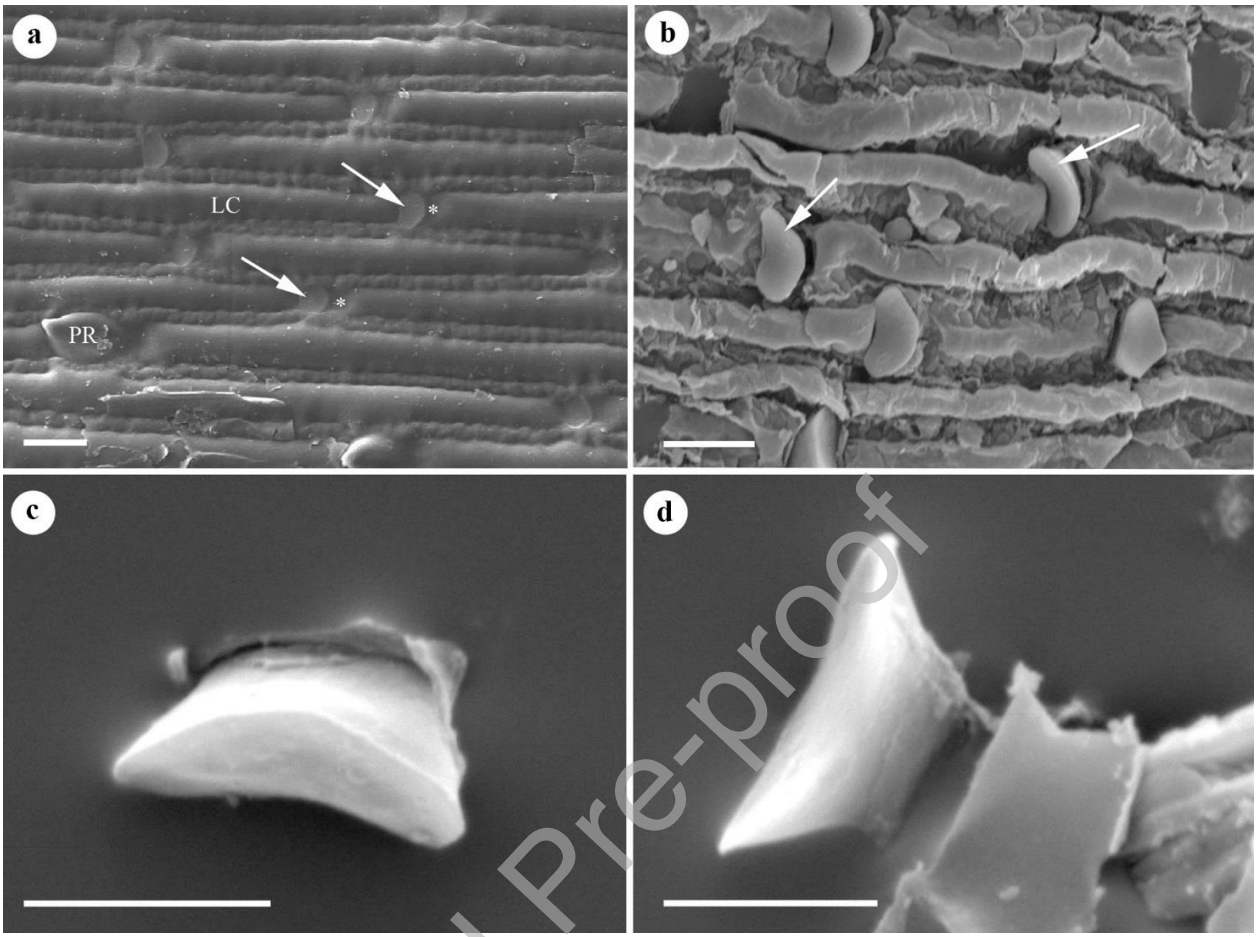

Fig. 3. SEM observations on *Festuca exaltata* leaf (a) YL stage. The disposition of the long cells with respect to the cork cells (asterisk) and the silica cells (white arrow) is shown. Two prickles (PR) are visible. SEM. Bar = 10 µm. (b) Leaf epidermis after charring. Note the position of phytoliths with the larger base (arrow) facing the outer part of the leaf. SEM image. Bar = 10 µm. (c) Single silica body. SEM. Bar = 10 µm. (d) Single silica body. SEM. Bar = 10 µm

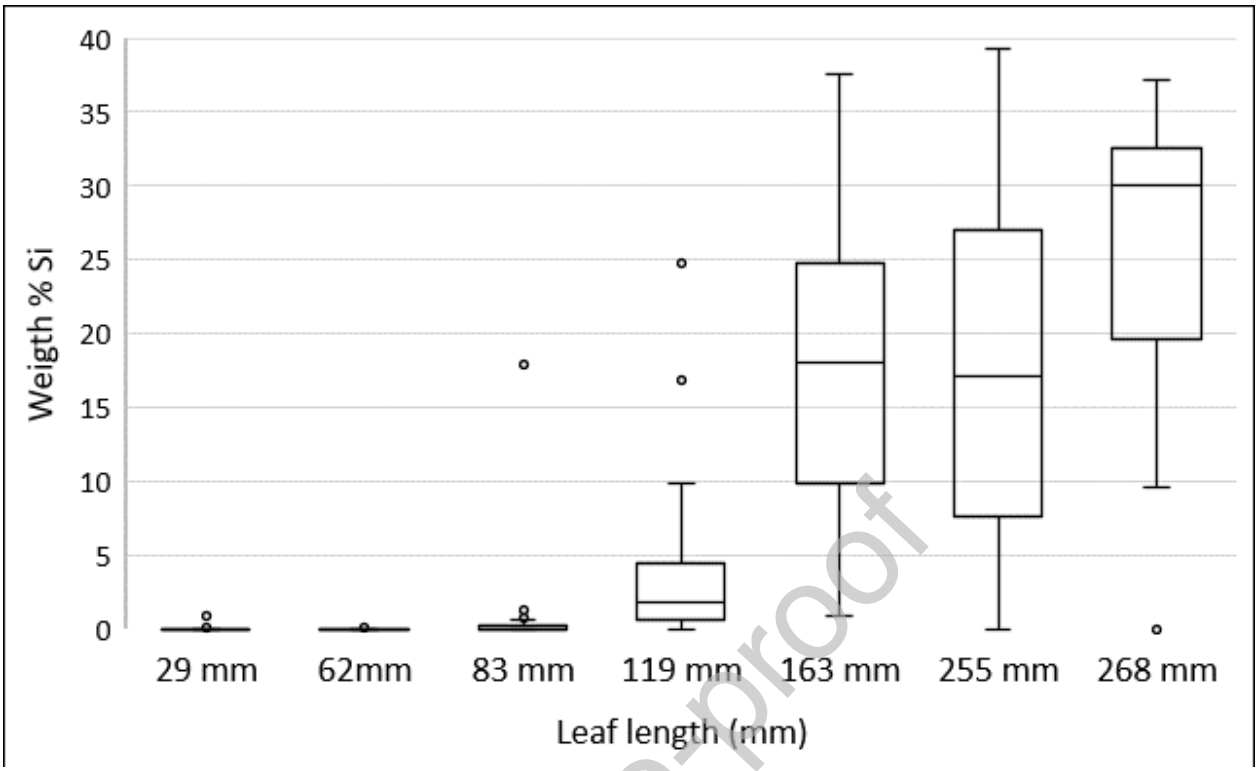

Fig. 4. Percentages of silica (weight % Si) in silica cells of *Festuca exaltata* leaves at different stages of development. Leaf length is reported on the x-axis. Note the increase of the content from young leaves (29, 62 and 83 mm) and unrolling leaves (119 mm) to well-developed leaves (163, 255, 268 mm). Box: median ± 1 quartile, whiskers = non-outlier values, < 1st quartile and > 3rd quartile, circles = isolated values and outliers

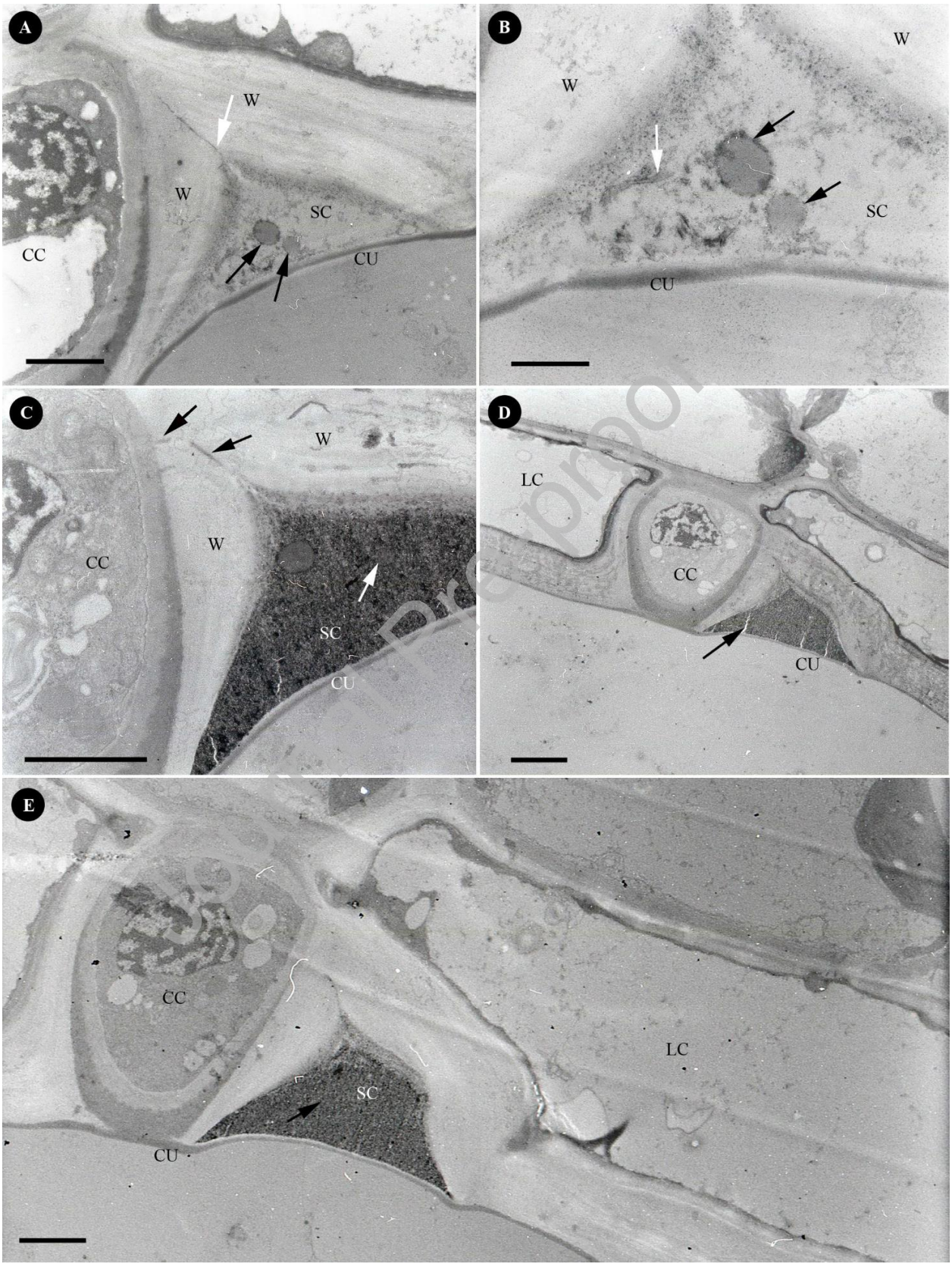
A
W
W
SC
CC
CU
B
W
W
SC
CU
C
W
W
CC
SC
CU
D
LC
CC
CU
E
CC
LC
SC
CU

Fig. 5. TEM observations on *Festuca exaltata* leaf, abaxial side. (a) YL stage. The silica cell cytoplasm contains some large spheroidal membrane-limited bodies (black arrows) containing a grey material. A channel is clearly observed connecting the internal tangential side of the silica cell to the cork cell (white arrow). The cork cell has electron dense cytoplasm, a nucleus with a condensed chromatin and a large vacuole. Bar = 2 µm (b) YL stage. Detail of the large spheroidal membrane-limited bodies (black arrows) in the silica cell cytoplasm. RER cisternae (white arrow) are visible close to the internal tangential wall. Bar = 2 µm (c) UL stage. The silica cell cytoplasm is occupied by a granular matrix (white arrow) tending to fracture along lines orthogonal to the external wall. The cork cell shows a thick wall and more electron dense layers are visible on the external tangential walls, while the nucleus has mainly condensed chromatin. Apparently a curved channel (black arrows) is apparently connecting the silica cell with the cork cell. TEM. Bar = 2 µm (d) DL stage. The silica cell cytoplasm is occupied by a granular matrix tending to fracture along lines orthogonal to the external wall (black arrow). The cork cell shows a thick wall, more electron dense layers are visible on the external side of the walls, while the nucleus has mainly condensed chromatin. Some chloroplasts of the underlying parenchyma are located close to the side of the silica cell, protruding towards the internal side of the mesophyll. Bar = 2 µm. (e) DL stage. The silica cell cytoplasm is occupied by a granular matrix (black arrow). No spheroidal membrane-limited body is visible in the cytoplasm. Bar = 2 µm. CC = cork cell, CU = cuticle, LC = long cell, SC = silica cell, W = wall

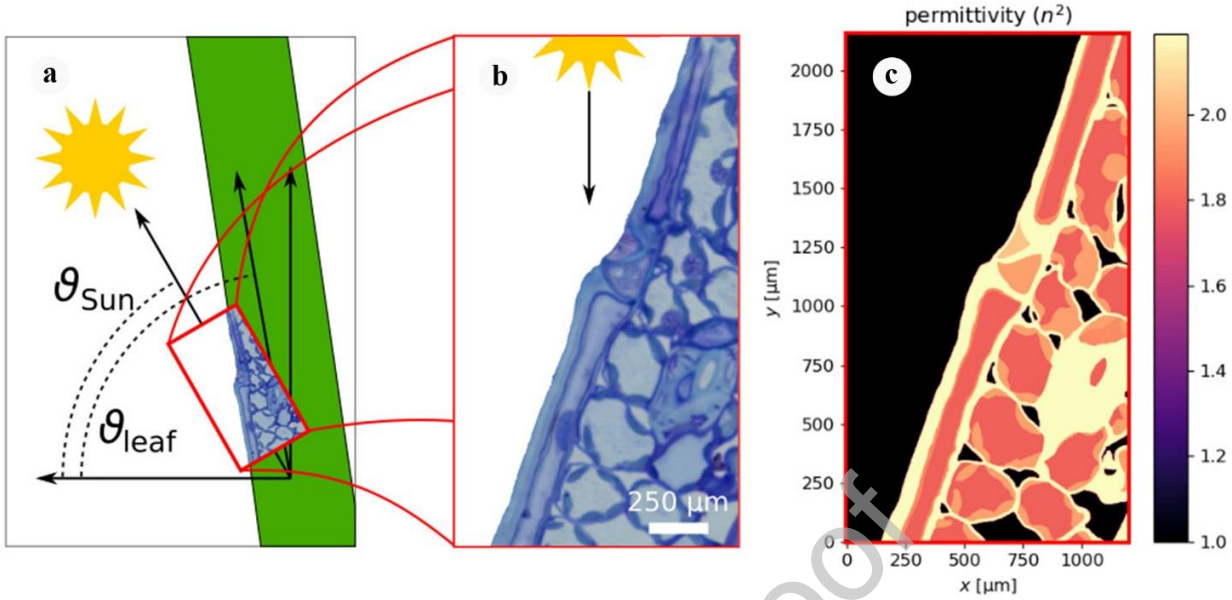

Fig. 6 Setup of numerical calculation (a) Sketch of typical leaf orientation. A region of interest on the lower side of the leaf is isolated from (b) an optical micrograph and rotated at different angles to simplify numerical calculations by allowing illumination from the vertical direction. Different regions are identified and segmented to form (c) a simplified representation of the permittivity distribution of the elements of the leaf epidermis and its underlying parenchyma.

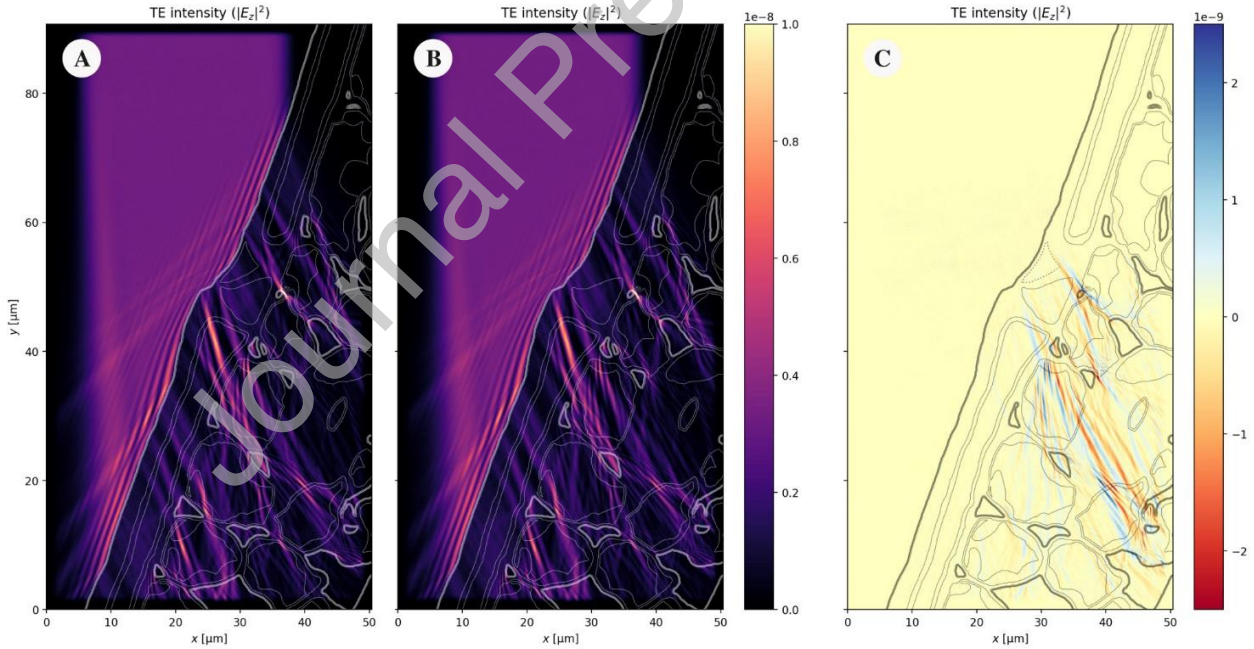

Fig. 7 Comparison between light intensity distributions in the epidermis (a) with the phytolith and (b) without the phytolith. Light intensity is shown in arbitrary units for TE polarization. Panel (c) shows the difference between the two (note the 4× enhancement of the colour bar limits to obtain an appreciable contrast).

Table 1. Main characteristics of the three main stages of development of the sampled leaves.

Stage	**Description**	**Leaf length**
YL (Young Leaves)	before unrolling, erect	3–8 cm
UL (Unrolling Leaves)	during the unrolling process, erect	about 12 cm
DL (Developed Leaves)	completely unrolled leaves, from erect to slightly patent (about 20 degrees from the vertical)	16–27 cm